

Article

Probabilistic Forecast and Risk Assessment of Flash Droughts Based on Numeric Weather Forecast: A Case Study in Zhejiang, China

Jinhua Wen¹, Yian Hua^{1,2}, Chenkai Cai^{1,*}, Shiwu Wang¹, Helong Wang^{1,3}, Xinyan Zhou¹, Jian Huang¹ and Jianqun Wang²

¹ Zhejiang Institute of Hydraulics and Estuary, Hangzhou 310020, China

² College of Hydrology and Water Resources, Hohai University, Nanjing 210098, China

³ College of Civil Engineering and Architecture, Zhejiang University, Hangzhou 310058, China

* Correspondence: chkcai@outlook.com

Abstract: In recent years, flash droughts with a rapid onset and strong intensity have attracted extensive attention due to their impact on agriculture and ecosystems. However, there is still no feasible method for flash drought forecasting and early warning. This paper employs the thresholds of several meteorological variables to identify flash droughts in Zhejiang Province, China, and build a probabilistic flash drought forecasting model through numeric weather forecast (NWF) and the generalized Bayesian model (GBM). The results show that the northern part of Zhejiang Province has the highest risk of flash drought. The NWF is a viable method to provide future information for flash drought forecasting and early warning, but its forecasting accuracy tends to decline with the increase in the lead time and is very limited when the lead time is over 5 days, especially for the precipitation forecast. Due to the low performance of the NWF, the flash drought forecast based on the raw NWF may be unreliable when the lead time is over 5 days. To solve this problem, probabilistic forecasting based on GBM is employed to quantify the uncertainty in the NWF and is tested through an example analysis. In the example analysis, it was found that the probability of a flash drought exceeds 30% from the probabilistic forecasting when the lead time is 12 days, while the deterministic forecasting via the raw NWF cannot identify a flash drought when the lead time is over 5 days. In conclusion, probabilistic forecasting can identify a potential flash drought earlier and can be used to evaluate the risk of a flash drought, which is conducive for the early warning of flash droughts and the development of response measures.

Keywords: flash drought; numeric weather forecast model; probabilistic forecast; Bayesian theory; Zhejiang Province



Citation: Wen, J.; Hua, Y.; Cai, C.; Wang, S.; Wang, H.; Zhou, X.; Huang, J.; Wang, J. Probabilistic Forecast and Risk Assessment of Flash Droughts Based on Numeric Weather Forecast: A Case Study in Zhejiang, China. *Sustainability* **2023**, *15*, 3865. <https://doi.org/10.3390/su15043865>

Academic Editor: Ozgur Kisi

Received: 17 January 2023

Revised: 10 February 2023

Accepted: 16 February 2023

Published: 20 February 2023



Copyright: © 2023 by the authors. Licensee MDPI, Basel, Switzerland. This article is an open access article distributed under the terms and conditions of the Creative Commons Attribution (CC BY) license (<https://creativecommons.org/licenses/by/4.0/>).

1. Introduction

Drought is one of the major natural disasters with high frequency, long duration, and wide impact across the world [1–3]. With the intensification of global climate change, the intensity and frequency of droughts have significantly increased. A drought does not only affect the ecological environment, but also threatens national food security [4–6]. Generally, a drought is considered as a slow developing natural phenomenon, which usually takes months or even longer to reach a certain degree in intensity and area, hence it would be clearly perceived by people [7,8]. However, recent studies have pointed out that drought can develop in a more intense and faster manner under the conditions of abnormal atmospheric circulation characteristics and certain land cover, and this phenomenon is called flash drought [9]. As a special form of drought event, the main difference between a flash drought and a conventional drought is the former's rapid development and short duration [10]. The sudden-onset nature of flash droughts makes it more difficult to provide early warning and prepare effective countermeasures for managers and stakeholders,

resulting in more severe impacts on agricultural production and ecosystems [11]. For instance, the drought that occurred in the U.S. Midwest in 2012, which was caused by a sudden high temperature and severe soil water depletion, was considered a typical flash drought event and led to a remarkable damage in the local agricultural production [12].

The concept of flash drought was first proposed in 2002 to describe a rapidly developing drought caused by severe heat wave and short-term drying [13], and many studies have been undertaken to identify, monitor, and evaluate flash drought events [14]. However, there is still no consistent standard to recognize and define flash droughts. Many previous studies have defined and recognized a flash drought based on the combination of thresholds from several hydrological and meteorological variables. Mo and Lettenmaier indicate that there are two types of flash drought: precipitation deficit flash drought and heat wave flash drought, which are caused by negative precipitation anomalies and heat wave respectively [15,16]. Other studies have suggested that the changing rate of hydrometeorological variables should also be taken into consideration in the definition of flash drought. One representative definition was proposed by Ford and Labosier [17], who defined a flash drought as soil moisture reductions from above the 40th percentile to below the 20th percentile within four pentads. Moreover, some traditional drought indices have been used to recognize flash drought, including the Evaporative Stress Index (ESI) and the Standardized Precipitation Evaporation Index (SPEI) [18,19]. In the literature, precipitation, temperature, soil moisture, and evaporation are considered as the most relevant measurements to flash drought and commonly used in studies with different spatio-temporal scales [20,21].

Another main concern of flash drought research is the forecasting and early warning of flash drought [22]. An accurate flash drought forecast model can help managers to formulate response measures in advance and reduce the impact of a flash drought. Numerous hydrometeorological models and statistical models have been employed to monitor and simulate flash droughts [23–25]. However, most of these studies have been more concerned with simulating the long-term evolution of the flash drought and identifying the key driving factors in the progress, and an effective method for the real-time forecasting and early warning of flash drought is still lacking [26]. Moreover, many researchers have indicated that climate change has increased the temperature of the land surface [27]. Higher temperatures and more frequent heat waves provide a favorable environment for flash droughts, which lead to a rising trend in the risk of flash droughts for many areas [28]. Considering the significant impact of a flash drought on agricultural, forestry, and ecosystem security, it is an urgent task to develop a flash drought forecasting model to assess the risk of flash drought under the changing environment. In addition, it is also worth noting that flash droughts are regarded as being caused by the joint effect of multiple hydrometeorological variables rather than a single variable alone, which makes the problem more complex [26,29].

With the development of meteorology, the performance of the medium- and long-range numerical weather forecast (NWF) has been improved in the past decade, which provides an opportunity for the real-time forecasting and early warning of flash droughts [30]. As a quantitative and objective method, the NWF can predict the future atmospheric conditions by mathematical models based on the initial weather conditions, including dozens of meteorological variables, such as precipitation, temperature, and evaporation. However, due to the chaotic nature of the meteorological system, the error and uncertainty of the NWF are still inevitable, especially when the lead time (i.e., the time interval between the initiation and the completion of a forecast process) is over 7 days [31]. The early warning and forecasting of a flash drought via NWF may be unreliable, and it is necessary to describe the uncertainty in flash drought forecasting based on the NWF. Many previous studies have pointed out that the post-processor for probabilistic forecasting is an effective way to improve the performance of the NWF and describe the uncertainty [32–34]. Although the probabilistic post-processors of a single variable from NWF have been commonly used in hydrological research, there has been limited study on the employment of probabilistic post-processors in flash drought early warning and forecasting, which are affected by

multiple variables. It still remains unknown whether the probabilistic NWF can be used to analyze the risk of flash droughts and as a reference for formulating countermeasures.

The main aim of this paper is to develop a probabilistic forecast model for flash drought forecasting and early warning based on the NWF and the probabilistic forecast. In this paper, the NWF from the Sub-seasonal to Seasonal Prediction (S2S) dataset is employed, and Zhejiang Province of China is selected as the study area. As a first step, we define an indicator to distinguish the meteorological flash droughts of the study area based on several thresholds of variables. Then, the performance of the NWF is evaluated through different evaluation indices. Finally, a probability forecast model for meteorological flash drought is built using uncertainty analysis.

2. Methodology

2.1. Flash Drought Identification

Since there is no consistent definition of flash drought, the first step of this study was to adopt a method to identify flash droughts [35,36]. In this paper, we followed the method from Mo and Lettenmaier [15,16], and identified flash droughts by thresholds of hydrometeorological variables. According to the former studies, the daily precipitation and daily average temperature were selected as the recognizers of flash droughts. The main reason for using these two variables are as follows: (1) These two variables are generally considered as the main meteorological forcing factors for changes in soil moisture, evaporation, and other hydrological factors. (2) Compared to soil moisture and evaporation, both precipitation and temperature have more reliable long-series ground-measured data, which is conducive to analyzing the accuracy of meteorological factors. In this paper, the thresholds of the two variables were forecasts and establishing a meteorological probabilistic forecasting model. According to this definition, flash droughts can be identified through

$$P_{acc} \leq P_{th} \text{ and } T_{avg} \geq T_{th} \quad (1)$$

where P_{acc} represents the accumulated precipitation for a pentad, T_{avg} represents the average temperature for a pentad, and P_{th} and T_{th} are the thresholds for the pentad accumulated precipitation and average temperature, respectively.

In this paper, the thresholds of the two variables were determined according to the long-term measured data and the historical reports, that is, $P_{acc}\% < 40\%$ and T_{avg} anomaly greater than 1.75 times the standard deviation.

2.2. Probabilistic Forecast for Flash Droughts

NWF is a method for weather forecasting that describes the progress of the meteorological system based on a set of equations and has been widely employed in hydrometeorological studies. However, a fundamental problem of NWF is the chaotic nature of the governing equations of atmosphere, which make it impossible to solve the equations exactly, and the forecast error cannot be ignored for the subseasonal to seasonal range [37]. Therefore, uncertainty generally exists in flash drought forecasting based on the NWF, which may lead to a wrong assessment of the flash drought risk and cause damage to agriculture, forestry, and ecosystems. Probabilistic forecasting based on uncertainty analysis has been proven to be an effective way to improve the forecasting skill of the NWF. It is necessary to describe the uncertainty in flash drought forecasting via probabilistic forecasting.

2.2.1. Generalized Bayesian Model

The generalized Bayesian model (GBM) developed by Cai et al. is a general post-processor to generate probabilistic meteorological forecasting from a single-value raw NWF [38]. There are three main steps to build the model: (1) deriving the prior distribution based on historical data; (2) obtaining the likelihood function based on the forecast errors; and (3) generating the conditional distribution of observation when the raw forecast value is provided. A brief introduction to the GBM is provided as follows.

As the first step, the marginal distribution of the P_{acc} and T_{avg} based on long-term measured data can be used as the prior distribution. Let Y_P represent the random variable (r.v.) for P_{acc} and Y_T represent the r.v. of T_{avg} . It is worth noting that the Y_T is a continuous r.v. with the range of $(-\infty, +\infty)$, while the Y_P is a mixed r.v. consisting of a discrete part and a continuous part with the range of $[0, +\infty)$. The discrete part of the Y_P is the probability of no rain (i.e., $Y_P = 0$), which can be estimated by the proportion of the number of no-rain days in the total number of days observed. The continuous part is for $Y_P > 0$ and can be described as a non-negative distribution. Therefore, the CDF of Y_P can be described as

$$F(y_P) = P\{Y_P \leq y_P\} = \begin{cases} 0, & y_P < 0 \\ P\{Y_P = 0\} + P_p\{Y > 0\} \cdot P\{0 < Y_P < y_P | Y_P > 0\}, & y_P > 0 \end{cases} \quad (2)$$

where $F(y_P)$ is the CDF of Y_P , and $P\{Y_P = 0\}$ is the probability of no-rain.

For the mixed distribution, as for Y_P , many traditional statistical analysis methods are not suitable, such as the Bayesian formula. In this paper, the generalized probability density function (GPDF) from the GBM was employed to solve this problem. The GPDF of Y_P can be written as Equation (3). More detailed information about the GPDF of GBM can be found in [25,30].

$$f_{Y_P}(y_P) = \alpha_0 \delta(y_P) + (1 - \alpha_0) f_{Y_P}(y_P | Y_P > 0) \quad (3)$$

where $f_{Y_P}(y_P | Y_P > 0)$ is the conditional probability density function (PDF) for $Y_P > 0$, and $\alpha_0 = P\{Y_P = 0\}$.

The prior distribution for Y_P can be expressed by the GPDF in Equation (3), while the prior distribution of Y_T is continuous r.v., which can be directly described by the PDF.

The second part of the GBM is the likelihood functions, which can be estimated by the forecasting error of the r.v. Let X_P and X_T represent the forecasted P_{acc} and T_{avg} , respectively. x_P and x_T denote the specific values of X_P and X_T , respectively. In the GBM, when $Y_P = y_P$ or $Y_T = y_T$ is provided, the relationship between the forecasting error and the forecasted values can be written as

$$\begin{aligned} X_P &= y_P + \varepsilon_P(y_P) \\ X_T &= y_T + \varepsilon_T(y_T) \end{aligned} \quad (4)$$

where $\varepsilon_P(y_P)$ and $\varepsilon_T(y_T)$ represent the forecast error.

From Equation (4), the likelihood functions, $f_{X_P|Y_P=y_P}(X_P | Y_P = y_P)$ and $f_{X_T|Y_T=y_T}(X_T | Y_T = y_T)$, can be derived by the distribution of ε_P and ε_T , respectively. Finally, the posterior distribution can be calculated by the following formula

$$f_{Y|X}(y|X = x) = \frac{f_Y(y) f_{X|Y}(x|Y = y)}{\int_{-\infty}^{+\infty} f_Y(t) f_{X|Y}(x|Y = t) dt} \quad (5)$$

where Y is the r.v. of the true value for the variable to be forecasted (i.e., the true value for P_{acc} and T_{avg} in this study), and X is the r.v. of the forecasted value for the NWF (i.e., the forecasted value for P_{acc} and T_{avg} in this study).

2.2.2. Probabilistic Flash Drought Forecasting

From the GBM, the probabilistic forecasting for P_{acc} and T_{avg} can be generated when the forecast value is provided. Then, let $f_{Y_P|X_P}(Y_P | X_P = x_P)$ and $f_{Y_T|X_T}(Y_T | X_T = x_T)$ represent the results from the GBM for P_{acc} and T_{avg} , respectively. Since the correlation coefficient between P_{acc} and T_{avg} is quite low, we assumed that the two variables were

independent. Therefore, the probability of a flash drought when the NWF is provided can be calculated by:

$$\begin{aligned}
 P_{FD} &= F(Y_P < P_{th}, Y_T > T_{th} | X_P = x_P, X_T = x_T) \\
 &= F(Y_P < P_{th} | X_P = x_P) \cdot F(Y_T > T_{th} | X_T = x_T) \\
 &= \int_0^{P_{th}} f_{Y_P | X_P}(t | X_P = x_P) dt \cdot \left(1 - \int_0^{T_{th}} f_{Y_T | X_T}(t | X_T = x_T) dt \right) \quad (6)
 \end{aligned}$$

where P_{FD} is the probability of a flash drought.

2.3. Verification Methods

In order to evaluate the performance of the meteorological forecast, several different indicators were employed in this paper, including the root-mean-square error (RMSE) and the correlation coefficient (CC). All the indicators were determined by the following equations:

$$RMSE = \sqrt{\frac{1}{N} \sum_{i=1}^N (x_i - y_i)^2} \quad (7)$$

$$CC = \frac{\sum_{i=1}^N (x_i - \bar{x})(y_i - \bar{y})}{\sqrt{\sum_{i=1}^N (x_i - \bar{x})^2 \sum_{i=1}^N (y_i - \bar{y})^2}} \quad (8)$$

where x_i and y_i denote the i th prediction and observation (true value), respectively, and N denotes the total number of forecasts and observations.

2.4. General Framework

The general flowchart of this study is shown in Figure 1. In this study, the measured data for precipitation and temperature were used to identify and define flash droughts, and the thresholds for the two variables for each grid were determined by the long-term measured data. Then, the performance of the NWF was evaluated by several different variables to show whether the uncertainty analysis for the NWF was necessary. Finally, a probabilistic flash drought forecasting model was established through GBM, and one main identified flash drought was used as an example to assess the accuracy of the model.

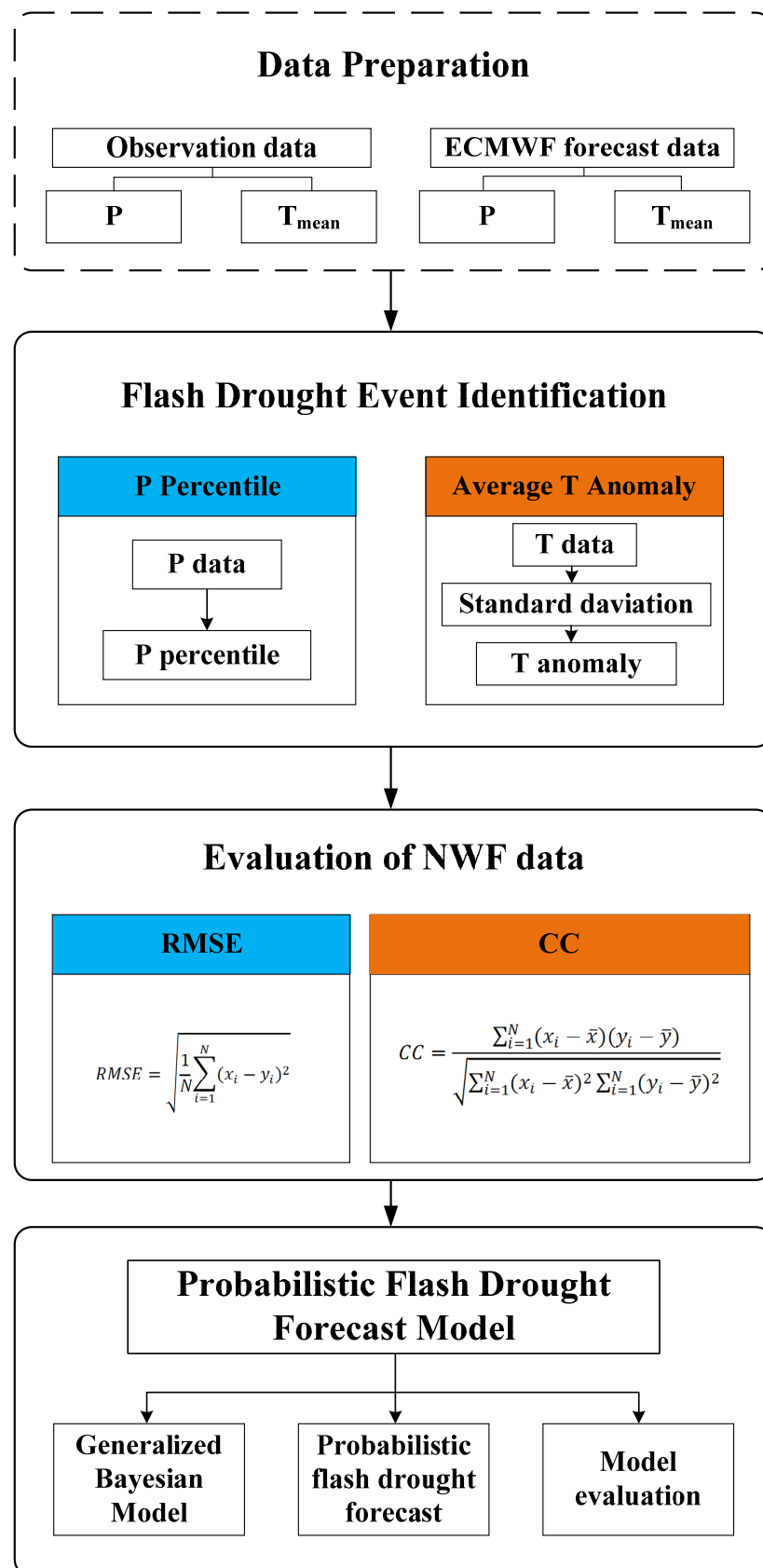


Figure 1. The flowchart of probabilistic flash drought forecasting and performance evaluation.

3. Study Area and Data Sources

3.1. Study Area

Zhejiang Province, located in the south-east of China (Figure 2), is one of the most developed and densely populated areas in China. From the digital elevation model (DEM) data in Figure 2, the area is mainly composed of mountains, hills, and plains, with the DEM decreasing from southwest to northeast. As a typical area affected by a monsoon climate, the area receives the highest precipitation and heat from April to September, which is conducive to agriculture. Due to its abundant water resources and suitable climate, Zhejiang Province plays an important role in the agricultural system of China. However, as influenced by climate change and human activities, the area has experienced several severe droughts in recent years, which have caused significant damage to agricultural production. Additionally, some studies have pointed out that China's southeast coastal areas will suffer more heat waves in the next 100 years based on the simulation of climate models [39,40]. Therefore, Zhejiang Province was selected as the study area in this paper to build an early warning model for flash droughts.

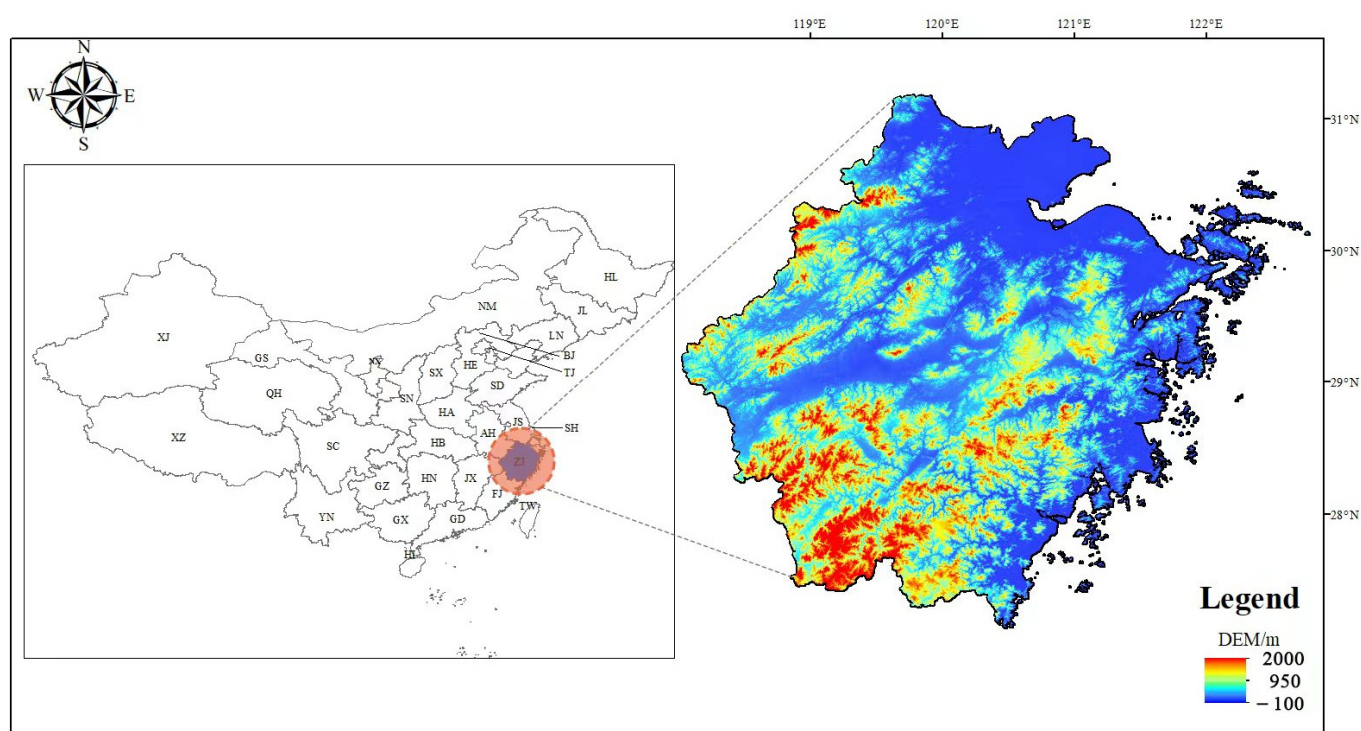


Figure 2. The location and DEM of Zhejiang Province.

3.2. Data Sources

As a joint research project of the World Weather Research Program (WWRP) and The Observing System Research and Predictability Experiment (THORPEX), the S2S dataset is an extensive data base of subseasonal (up to 60 days) forecasts and reforecasts based on the THORPEX Interactive Grand Global Ensemble (TIGGE) and the Climate System Historical Forecast Project (CHFP) [41,42].

The main aim of the S2S dataset is to improve the forecast skill and understanding of the weather forecast on a time scale from subseason to season and promote its application in extreme weather forecasting and early warning, such as droughts, floods, and heat waves. Currently, the NWF data from 12 meteorological centers from different countries or regions are contained in the S2S dataset. However, due to the different models and forcing data used by different meteorological centers, consensus still needs to be reached on how to produce these forecasts, including the start dates, the length of the forecasts, the averaging periods, and the update frequency of the forecasts. Therefore, the NWF

from the European Centre for Medium-Range Weather Forecasts (ECMWF) was selected as the data source in this paper to avoid the influence from different meteorological centers. Furthermore, the main reason why the TIGGE dataset, which is more frequently updated, was not selected in this paper was the lead time. The maximum lead time of the TIGGE dataset is 15 days [43]. Although the duration of a flash drought is generally short, it is still likely to exceed 15 days, which means this dataset would only play a limited role in the early warning of a flash drought and preparation of countermeasures.

The observed meteorological data used in this paper were from the dataset of the China meteorology agency. For a better comparison between the NWF and the observations, several methods were employed to make the two datasets consistent. (1) The base time of the NWF used in this study was 00:00UTC; (2) the forecast length for this study was 720 h (30 days); (3) the spatial resolution of the two datasets was both $0.5^\circ \times 0.5^\circ$; and (4) the observed data employed in this study were from 1964 to 2020, while the NWP data were from 2016 to 2020.

4. Results and Discussions

4.1. Flash Drought Identification for Zhejiang Province

As the first step of this study, the specific thresholds for the different grids in Zhejiang Province were determined from the long-term observations. Figure 3 shows the thresholds of the two variables. It can be found in Figure 3 that the threshold for P_{acc} showed a decreasing trend from south-west to north-east (Figure 3a), which was similar to the trend of the DEM (Figure 2). To be more specific, the threshold for the P_{acc} in the mountain and hill areas from the south-west was higher than that in the coastal areas dominated by the plains from the north-east. The maximum value for the threshold of the T_{avg} was shown in the north part of the study area, and the threshold in the southern part was relatively small (Figure 3b).

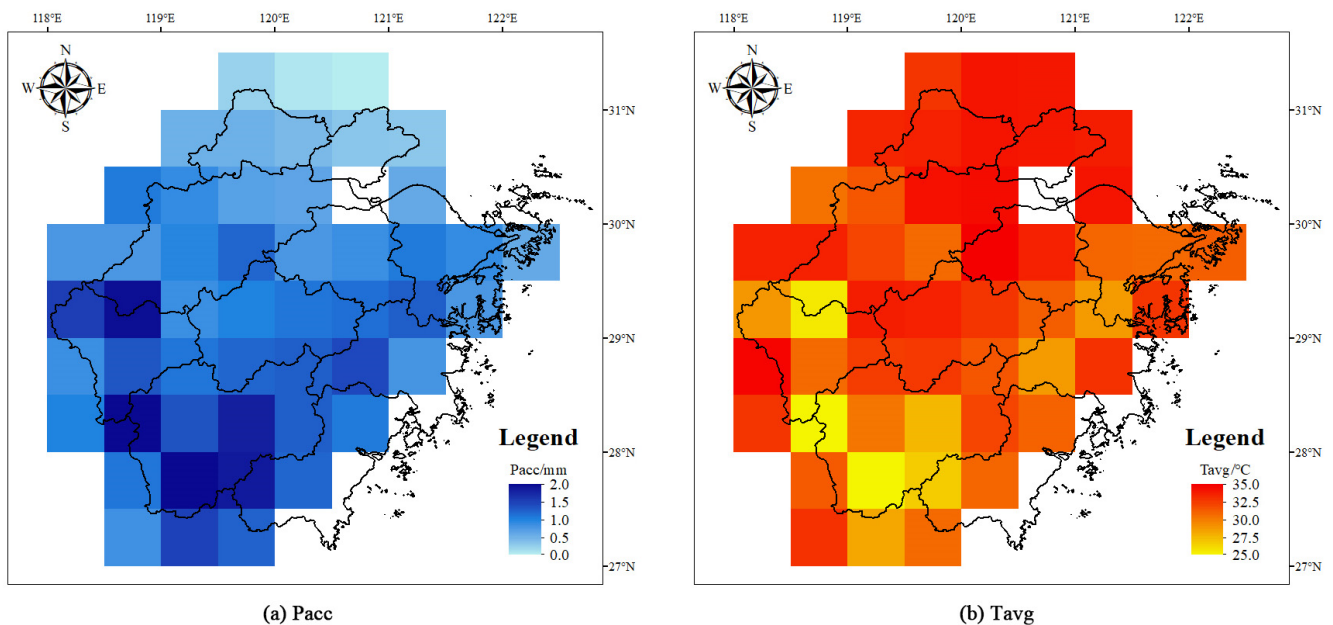


Figure 3. The spatial distribution of the thresholds for the P_{acc} and T_{avg} in the study area based on the measured data from 1964 to 2020 in Zhejiang Province. (a) The threshold for the P_{acc} . (b) The threshold for the T_{avg} .

The frequency and duration of the flash droughts during the entire time period are presented in Figure 4. From Figure 4a,b, we can see that the spatial distributions of the frequency and duration for flash droughts were quite similar in the study area. Historically, the frequency and total duration of flash droughts in the northern part of Zhejiang Province

were greater than those in the south. It is worth noting that, although the threshold for the P_{acc} was low (Figure 3a) and the threshold for the T_{avg} was high (Figure 3b) in the north of the study area, which means a more stringent standard, it still has the largest frequency and longest duration for flash drought in its history. Therefore, specific attention should be paid to this area for the risk of flash droughts. On the other hand, the probability of a flash drought in the south and coastal areas was obviously smaller, and several areas had never experienced a flash drought in their history.

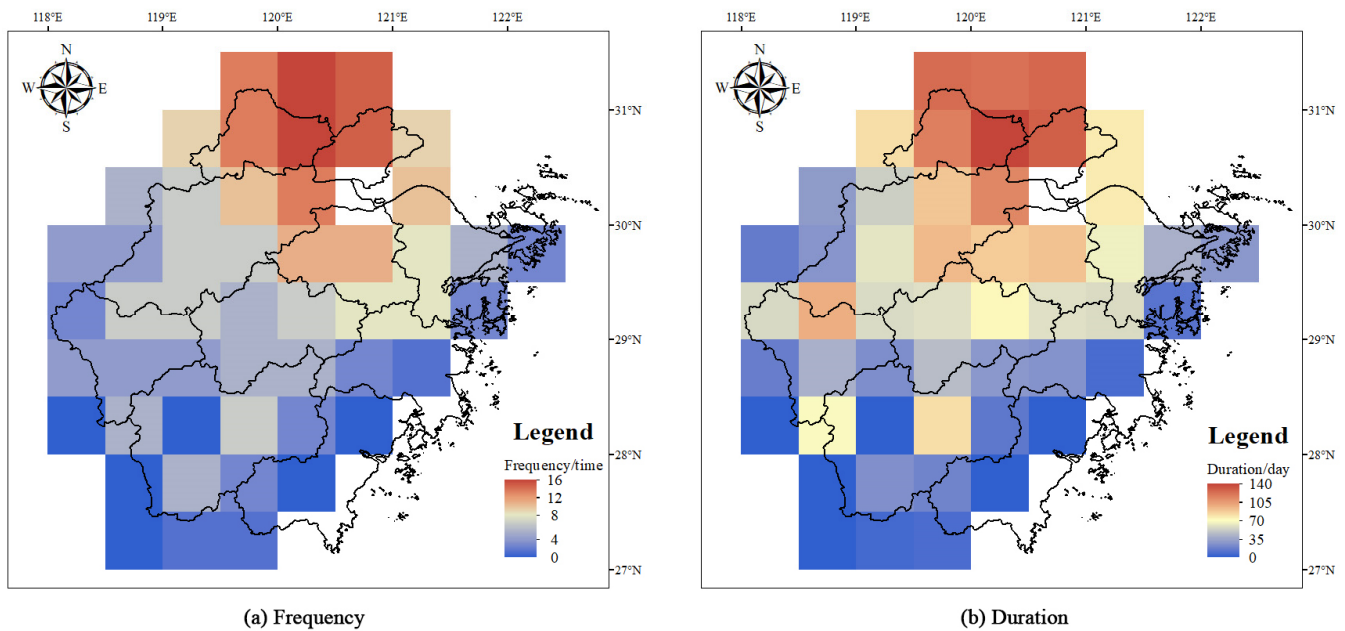


Figure 4. The frequency and duration of flash droughts in Zhejiang Province from 1964 to 2020. (a) The frequency of the flash droughts. (b) The duration of the flash droughts.

4.2. Performance Assessment of NWF

The second part of this study aimed to evaluate the performance of the NWF in Zhejiang Province. Firstly, the averages of the precipitation and temperature forecasts for the study area from different lead times were evaluated through the CC and RMSE, as shown in Figure 5. The performance of the CC for the two variables in the Figure 5a showed a downward trend as the lead time grew. Moreover, the CC of precipitation exhibited obvious fluctuations, while the results for the temperature were more stable. From Figure 5b, the temperature showed a quite similar performance, i.e., the RMSE had a very slight increase with the lead time. However, the RMSE of the precipitation showed more dramatic changes, especially when the lead time exceeded 3 days. To be more specific, the RMSE of the precipitation increased rapidly when the lead time was between 3 days and 5 days and remained relatively stable for the lead time over 5 days. Furthermore, the results in Figure 5 also indicate that the accuracy in forecasting the temperature is higher than for the precipitation.

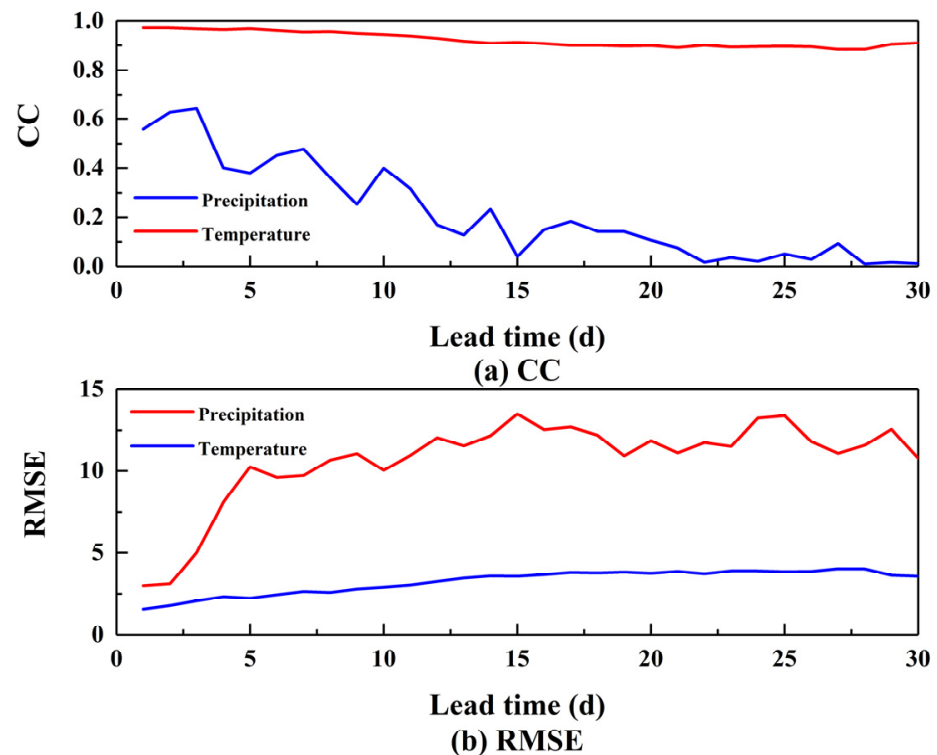


Figure 5. The performance of area-averaged NWF from different lead times. (a) CC and (b) RMSE.

Figures 6 and 7 show the spatial distribution of the CC and the RMSE for the precipitation forecast using the NWF, respectively. The performance of the precipitation forecast in the western part was more accurate when the lead time was within 20 days, while the eastern coastal areas performed better when the lead time was over 20 days. Moreover, the performances of the CC and RMSE were not similar, which means that a higher CC did not lead to a smaller RMSE for the precipitation forecast. The spatial distributions of the CC and RMSE for the temperature forecast are shown in Figures 8 and 9, respectively. From Figures 8 and 9, we can see that the spatial distributions of the CC and RMSE for the temperature forecast varied slightly with the change in the lead time. The temperature forecast in the north-eastern part, generally, had a better performance. The low CC and high RMSE were clear in the south-west of the study area. In addition, the spatial distributions of the CC and the RMSE also implied that the temperature forecast was more accurate than the precipitation forecast. The boxplots of CC and RMSE for the grids from different lead times are shown in Figures 10 and 11. The horizontal line in the box represents the median of the distribution (50% of the data are greater than this value), and the upper and lower box limits represent the upper and lower quartiles (25% of data greater/lower than the value), respectively. The top and bottom horizontal lines represent the maximum and minimum values of the two-thirds of the quantile, respectively. The outlier points show values more than two-thirds of the quantile. From Figures 10 and 11, the change trends of the RMSE and CC for the NWF with the lead time were more obvious. The distribution range of the boxes became larger with the increase in the lead time, except for the CC from the precipitation forecast, which means the accuracy of the NWF was unstable when the lead time exceeded a certain limit. According to the results from Figures 5–11, it can be found that the performance of the temperature forecast is better than that of the precipitation forecast, and the results from the precipitation forecast may be unreliable and lead to a false or missing alarm for a potential flash drought with the increase in the lead time.

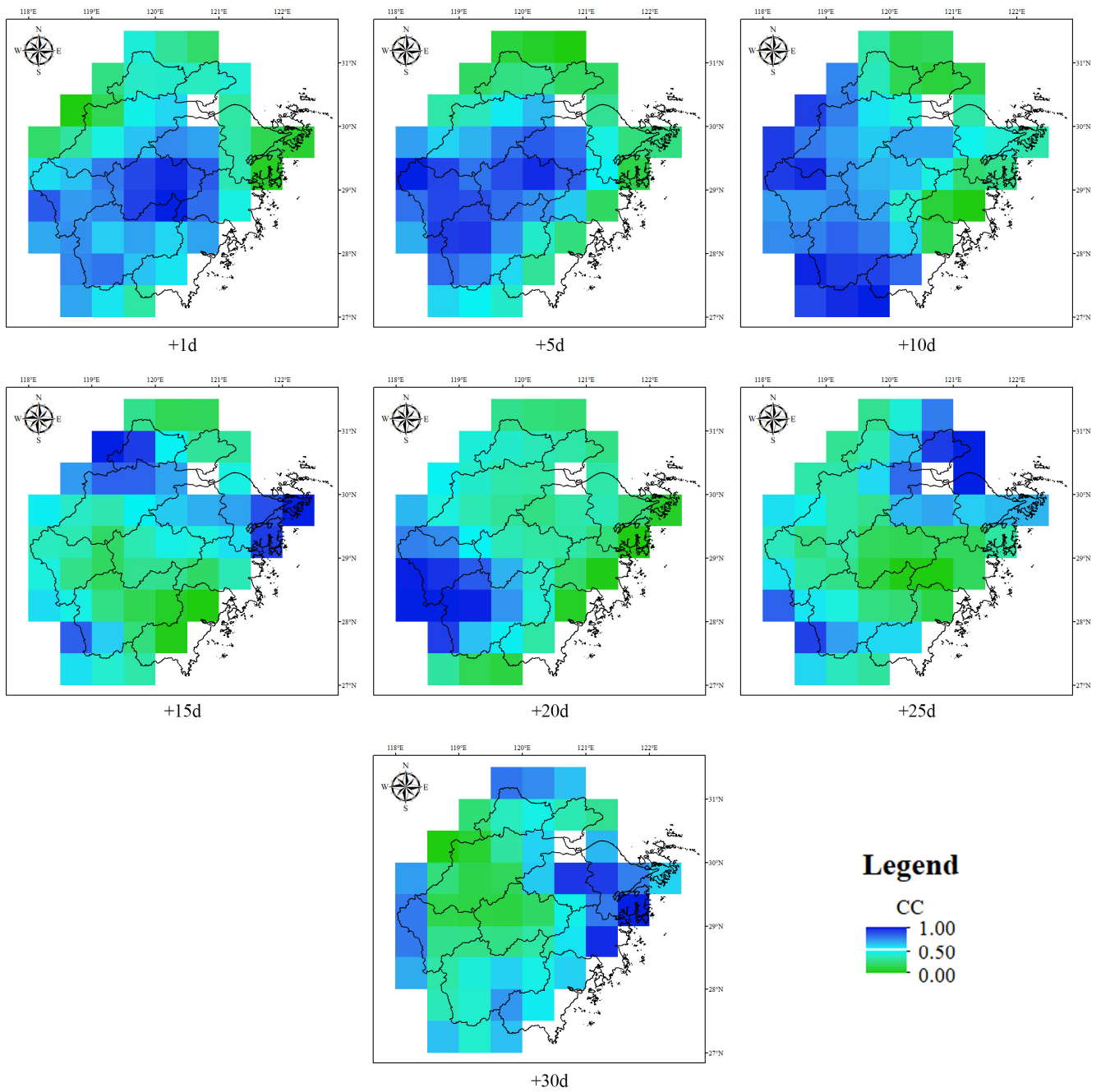


Figure 6. The spatial distribution of the CC for the precipitation forecast in the study area.

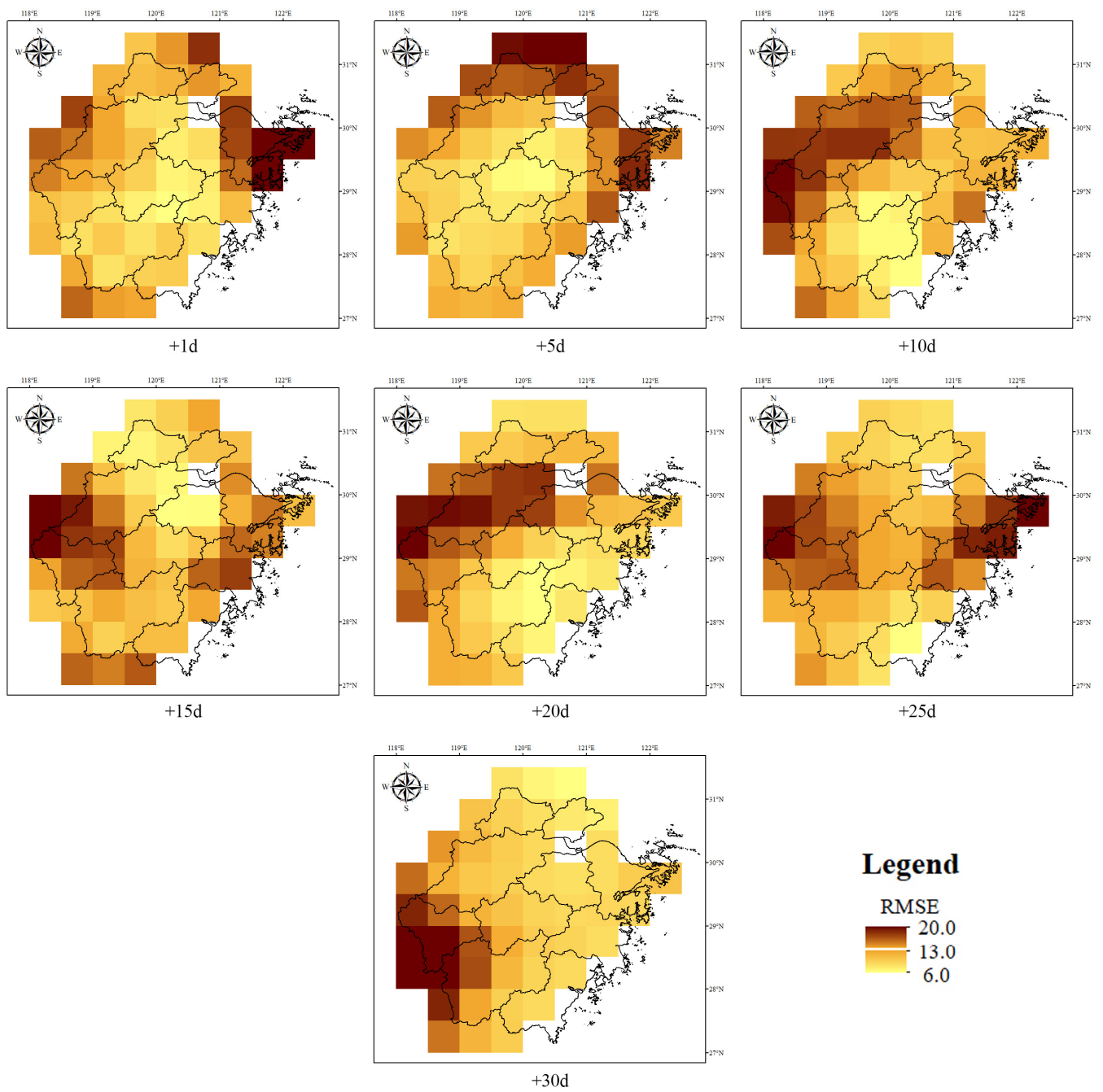


Figure 7. The spatial distribution of the RMSE for the precipitation forecast in the study area.

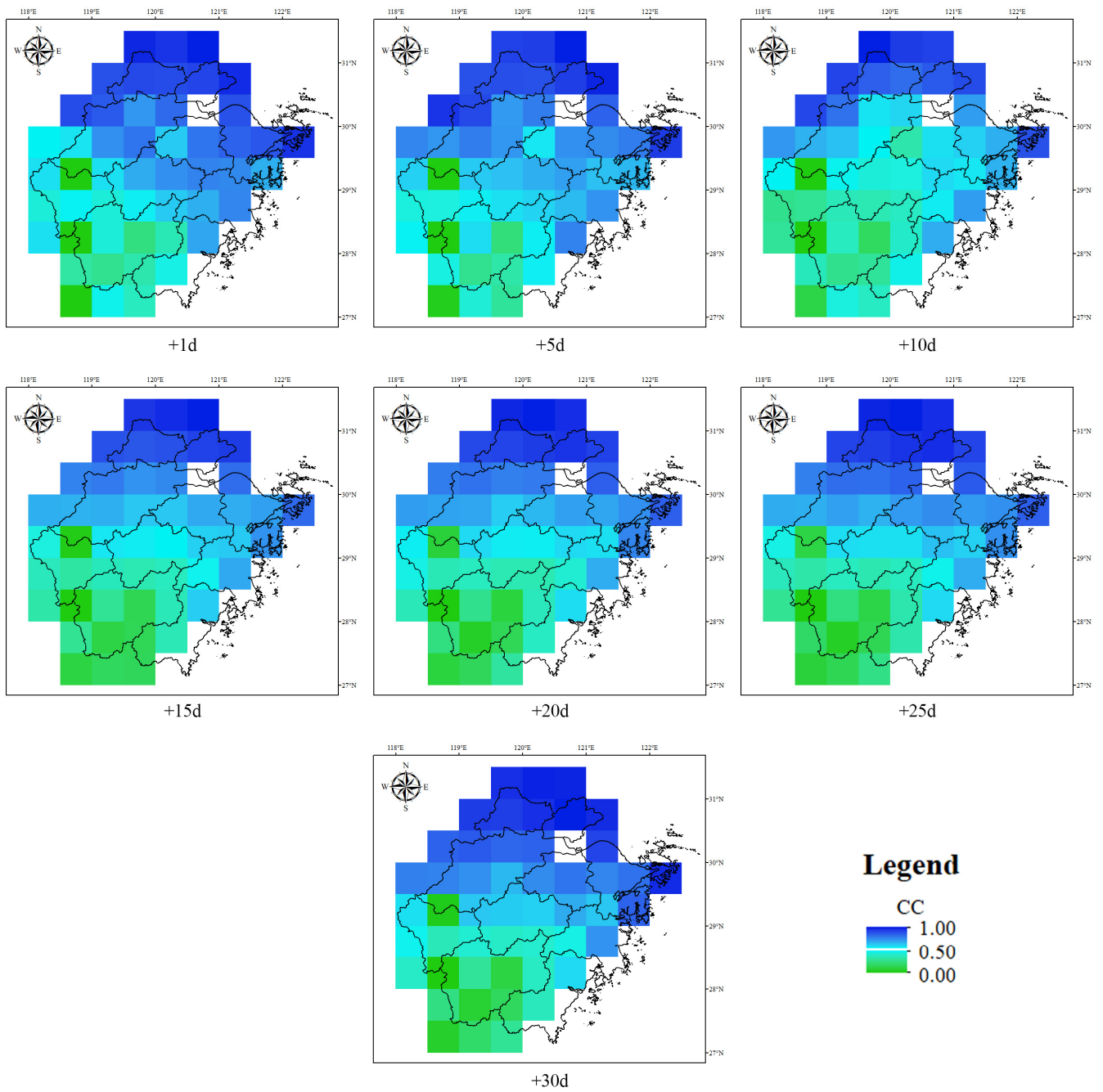


Figure 8. The spatial distribution of the CC for the temperature forecast in the study area.

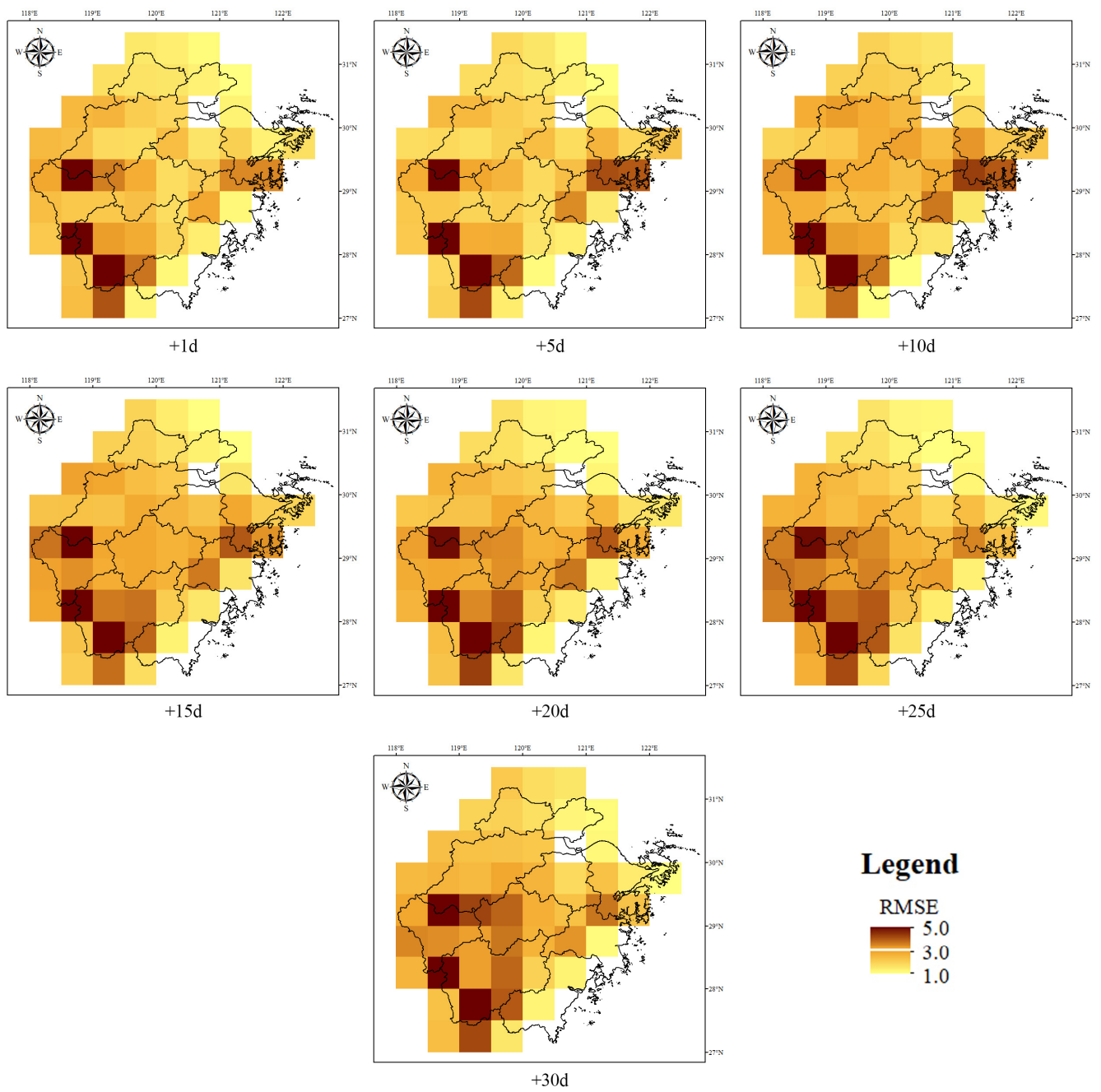


Figure 9. The spatial distribution of the RMSE for the temperature forecast in the study area.

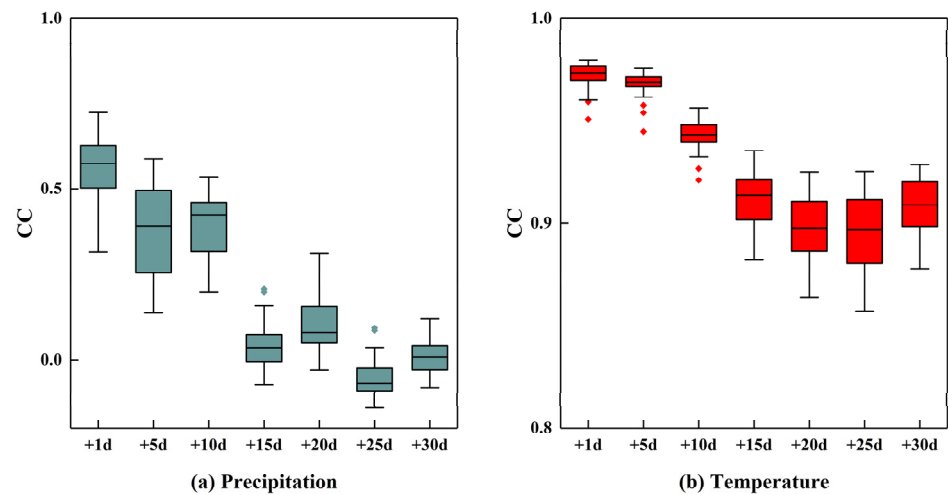


Figure 10. The boxplots of CC for the grids from different lead times.

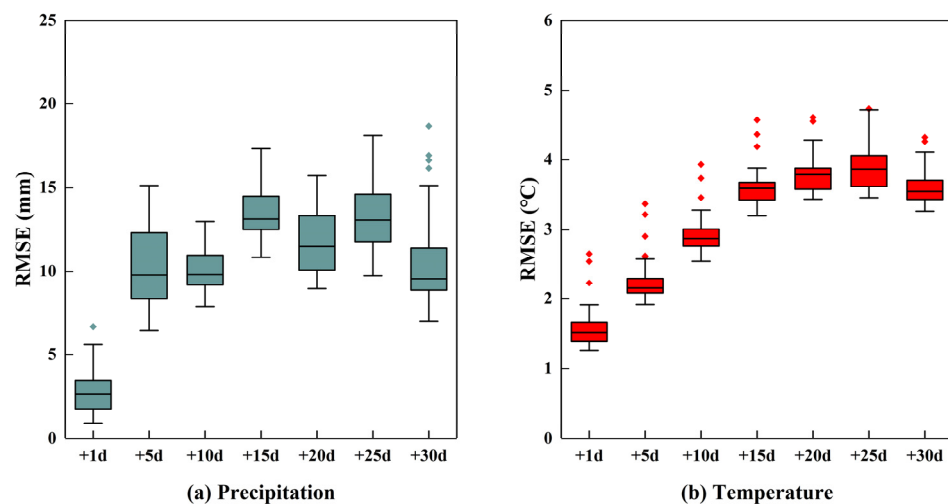


Figure 11. The boxplots of RMSE for the grids from different lead times.

4.3. Evaluation of Probabilistic Flash Drought Forecasting

To examine the effectiveness of probabilistic flash drought forecasting, a main flash drought event was selected as the example. The event occurred in the south-west of the study area from 22 July to 26 July 2016. Figure 12 shows the deterministic forecast results from different base times. It can be found in the figure that the precipitation forecast generally overestimated the precipitation, while the temperature forecast tended to underestimate the temperature. Compared to the results from the base time closer to the flash drought event, the forecasting results with a long lead time had a worse performance, which was consistent with the results from the evaluation of the NWP. The forecasting results from 7 July had the worst forecast skill, which greatly overestimated the precipitation and underestimated the temperature. As a commonly used index for forecast accuracy evaluation, the RMSE for the deterministic precipitation and temperature forecast are shown in Table 1. From Table 1, the RMSE for the precipitation and temperature forecast was from 0.2 to 1.1 mm and 1.4 to 4.3 °C, respectively. According to the definition of a flash drought in this paper, the forecasting results from the base times of 18 and 21 July successfully identified the flash drought event, while the others failed, which means the longest effective lead time for this event was only 5 days, which may not meet the demand of early warning for a potential flash drought event.

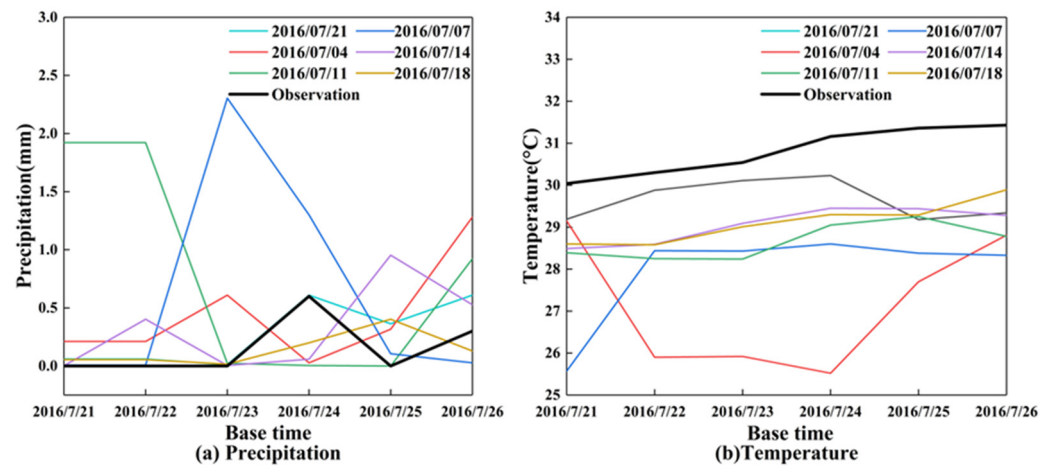


Figure 12. The deterministic precipitation and temperature forecasting results for the flash drought events from 22 July to 26 July 2016. (a) Precipitation and (b) temperature. Note that the x-label is the base time (i.e., the start time of the forecast).

Table 1. The RMSE of the raw NWF for the present example.

Base Time	RMSE	
	Precipitation (mm)	Temperature (°C)
04 July	0.60	1.44
07 July	1.09	4.31
11 July	0.94	2.57
14 July	0.53	2.25
18 July	0.27	1.80
21 July	0.22	1.76

For the short-term NWF, the model error is not usually so dominant, but for the subseasonal to seasonal range, the model error is too large to be ignored. Moreover, the results of the performance evaluation for the NWF show that the forecasting accuracy of the NWF is quite limited when the lead time is over 5 days, especially for the precipitation forecast. The statistical post-processors based on Bayesian theory have been proven as an effective way to improve the performance of the NWF and have been widely used in the studies for flood forecasting, which is known as probabilistic flood forecasting. Therefore, the GBM, an uncertainty analysis tool for precipitation and temperature forecasting, was employed to generate the probabilistic flash drought forecasting in this paper.

To show the difference between the probabilistic forecast and the raw NWF, the probability of a flash drought from different base times through the probabilistic forecast is shown in Figure 13 and a direct comparison between the two forecast results from different base times is presented in Table 2. Note that, since the results of the raw NWF were deterministic, the probability of a flash drought can only be 0 (if the forecast result does not fit the thresholds of flash drought) or 100% (if the forecast result fits the thresholds of flash drought). It can be also found in Table 2 that the probability of a flash drought with a short lead time was much higher than that with a long lead time. The increasing trend in the probability of flash drought is more evident, as shown in Figure 13, and the increasing trend gradually slowed as the base time changed. Compared to the results of the raw NWF, the probability of a flash drought based on probabilistic forecasting has better performance for a long lead time, but the performance was worse for the base time with a short lead time. Another main concern, discerned from Table 2, is that the accuracy of the probabilistic forecast with the long lead time was still quite low. The main advantage of the probabilistic forecast is that it can still provide the potential risk of a flash drought when the lead time exceeds 5 days, which is useful for the early warning of and preparation for flash

droughts. According to the probabilistic forecasting results, it is a feasible method to set a probability threshold based on the preferences of decision makers to determine whether a strategy for flash droughts should be prepared. For example, if the probability threshold is 30%, the effective lead time can be extended to 12 days since the probability of flash droughts surpassed 30% for the base time of 11 July. In practical application, probabilistic flash drought forecasting can provide more information about risks and should be analyzed in line with the preference of the decision-maker to formulate reasonable strategies for minimizing the impact of a flash drought.

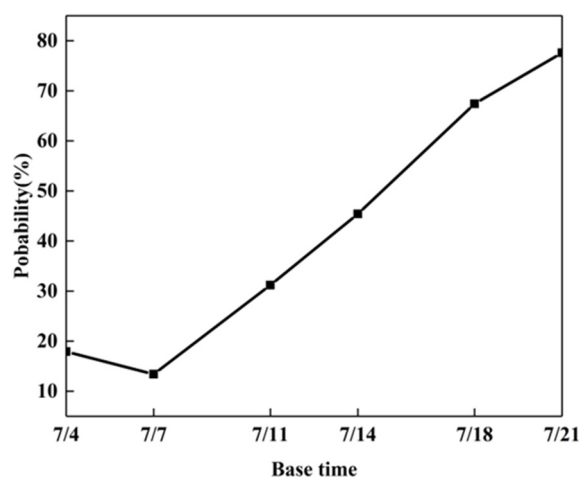


Figure 13. The relationship between the probability of a flash drought and the base time.

Table 2. The results from the probabilistic forecast and the raw NWF.

Base Time	Probability of Flash Drought (%)	
	Probabilistic Forecast	Raw NWF
04 July	17.9	0.0
07 July	13.4	0.0
11 July	31.2	0.0
14 July	45.4	0.0
18 July	67.4	100.0
21 July	77.6	100.0

4.4. Limitations and Future Work

In this paper, a probabilistic flash drought forecasting model was proposed based on the NWF and Bayesian theory. Compared to former studies on the simulation of flash droughts based on long-term data [22,28,40], more attention was paid to a real-time early warning and forecasting for a flash drought, which means this study had a smaller time scale, but required a higher accuracy. Of course, as with all scientific research, this study had several obvious limitations. Firstly, due to the lack of a consistent definition for a flash drought, the thresholds of precipitation and temperature were used to identify the flash drought in the study area. Although the thresholds were determined based on the long-term observed data and historical reports, we have to point out that these thresholds used in this study may not be suitable for all areas or basins, and the definition of flash drought should be determined according to the study's aim and actual situation. In addition, considering the availability of the observations, only two meteorological variables with coarse spatial resolution were used to identify the flash drought. With the rapid development of remote sensing, it is feasible to obtain more measured data of different meteorological variables with higher resolution through satellites in the future. However, more tests are still necessary to evaluate the performance of observations from satellites at present.

Another main limitation of this study was the performance of the NWF. Many researchers have indicated that the subseasonal NWF is an effective way to forecast a flash drought [44–46]. However, due to the nonlinearity of the atmospheric system, the accuracy of the NWF remained far from meeting the demand of an early warning for extreme hydrological events, which means the flash drought forecasting based on raw NWF may have a poor performance and cannot be used in practical applications. Probabilistic forecasting was used to improve the performance of NWF and provide more information through the probability distribution, but it was still difficult to assess the risk of a flash drought with a long lead time. The results of this study indicate that the early warning and forecasting of a flash drought based on the NWF is far from ready for practical applications. Fortunately, the accuracy of the NWF has been continuously improved over the past few decades and it may be possible to generate a more accurate probabilistic flash drought forecast based on the NWF in the future. Furthermore, former studies have pointed out that a multi-model ensemble forecast is also an effective way to improve the performance of the NWF and generate a better probabilistic forecast, which may be a feasible solution to improve the accuracy of probabilistic flash drought forecasting [47,48].

5. Conclusions

With the rapid population growth as well as climate change, the risk of flash droughts is rising in many areas. However, due to the lack of a unified definition, there is still no effective early warning or forecasting model for flash droughts. In this paper, a probabilistic flash drought forecasting model was proposed based on the thresholds of the hydrometeorological variables and the NWF, and Zhejiang Province was selected as a study case to examine the performance of the model.

First, the definition of a flash drought used in this study was determined according to the results of Mo and Lettenmaier. Considering the availability of the measured data and the physical significance of a flash drought, the thresholds of precipitation and temperature were used as the identifiers for a flash drought. According to the measured data of the study area, the risk of flash drought in the northern Zhejiang Province was higher, with a higher frequency and longer duration. The performance evaluation of the NWF indicated that the forecast accuracy of the precipitation and temperature decreased with the increase in the lead time, and the declining trend of the precipitation forecast was more significant. The post-processor based on uncertainty analysis is an effective way to improve the performance of the NWF. Therefore, the GBM was employed to generate a probabilistic flash drought forecast from raw the NWF. A main flash drought event in the study area was selected as an example to test the accuracy of the probabilistic forecast. The results show that probabilistic forecasting can provide more information about the flash drought and extend the lead time. To be more specific, based on the example analysis, the probability of flash drought through probabilistic forecasting exceeded 30% when the lead time was 12 days, while the effective lead time for deterministic forecasting was only 5 days. In other words, probabilistic forecasting can detect a potential flash drought earlier than deterministic forecasting, which is conducive to managers being able to release alerts and formulate corresponding strategies.

Author Contributions: Conceptualization, C.C.; methodology, J.W. (Jinhua Wen) and Y.H.; software, J.W. (Jinhua Wen); investigation, X.Z. and J.H.; data curation, Y.H., X.Z. and J.H.; writing—original draft preparation, J.W. (Jinhua Wen); writing—review and editing, C.C., S.W. and J.W. (Jianqun Wang); supervision, S.W. and J.W. (Jianqun Wang); funding acquisition, C.C., H.W. and S.W. All authors have read and agreed to the published version of the manuscript.

Funding: This study was supported by the Science and Technology Plan of Department of Water Resources of Zhejiang Province (RB2020 and RC2114), and President's Science Foundation of Zhejiang Institute of Hydraulics and Estuary (ZIHE22Q014 and ZIHE21Q005).

Institutional Review Board Statement: Not applicable.

Informed Consent Statement: Not applicable.

Data Availability Statement: The S2S datasets can be downloaded from <https://www.ecmwf.int/>, accessed on 1 January 2015. The observation data can be downloaded from <http://data.cma.cn/>, accessed on 1 January 2005.

Conflicts of Interest: The authors declare no conflict of interest.

References

1. Wilhite, D.A.; Glantz, M.H. Understanding the drought phenomenon: The role of definitions. *Water Int.* **1985**, *10*, 111–120. [[CrossRef](#)]
2. Mishra, A.K.; Singh, V.P. A review of drought concepts. *J. Hydrol.* **2010**, *391*, 202–216. [[CrossRef](#)]
3. Aghakouchak, A.; Farahmand, A.; Melton, F.S.; Teixeira, J.; Anderson, M.C.; Wardlow, B.D.; Hain, C.R. Remote sensing of drought: Progress, challenges and opportunities. *Rev. Geophys.* **2015**, *52*, 452–480. [[CrossRef](#)]
4. Apurv, T.; Sivapalan, M.; Cai, X. Understanding the Role of Climate Characteristics in Drought Propagation. *Water Resour. Res.* **2017**, *53*, 9304–9329. [[CrossRef](#)]
5. Dai, A. Drought under global warming: A review. *Wiley Interdiscip. Rev. Clim.* **2011**, *2*, 45–65. [[CrossRef](#)]
6. Dai, A. Increasing drought under global warming in observations and models. *Nat. Clim. Change* **2013**, *3*, 52–58. [[CrossRef](#)]
7. Crausbay, S.D.; Ramirez, A.R.; Carter, S.L.; Cross, M.S.; Hall, K.R.; Bathke, D.; Betancourt, J.; Colt, S.; Cravens, A.; Dalton, M.S.; et al. Defining ecological drought for the twenty-first century. *B Am. Meteorol. Soc.* **2017**, *98*, 2543–2550. [[CrossRef](#)]
8. Vicente-Serrano, S.M.; Quiring, S.M.; Peña-Gallardo, M.; Yuan, S.S.; Domínguez-Castro, F. A review of environmental droughts: Increased risk under global warming? *Earth-Science Rev.* **2020**, *201*, P102953. [[CrossRef](#)]
9. Otkin, J.A.; Svoboda, M.; Hunt, E.D.; Al, E. Flash droughts: A review and assessment of the challenges imposed by rapid-onset in the United States. *Bull. Amer. Meteor. Soc.* **2018**, *18*, 911–919.
10. Zhang, M.; Yuan, X. Rapid reduction in ecosystem productivity caused by flash drought based on decade-long FLUXNET observations. *Hydrol. Earth Syst. Sci.* **2020**, *24*, 5579–5593. [[CrossRef](#)]
11. Li, J.; Wang, Z.L.; WU, X.S.; Al, E. A new framework for tracking flash drought events in space and time. *Catena* **2020**, *194*, 104763. [[CrossRef](#)]
12. Hoerling, M.; Eischeid, J.; Kumar, A.; Al, E. Causes and predictability of the 2012 great Plains drought. *Bull. Amer. Meteor. Soc.* **2014**, *95*, 269–282. [[CrossRef](#)]
13. Svoboda, M.; LeComte, D.; Hayes, M.; Heim, R.; Gleason, K.; Angel, J.; Rippey, B.; Tinker, R.; Palecki, M.; Stooksbury, D.; et al. The drought monitor. *B. Am. Meteorol. Soc.* **2002**, *83*, 1181–1190. [[CrossRef](#)]
14. Liu, Y.; Zhu, Y.; Ren, L.L.; Otkin, J.A.; Hunt, E.D.; Yang, X.L.; Yuan, F.; Jiang, S.H. Flash droughts characterization over China: From a perspective of the rapid intensification rate. *Sci. Total Environ.* **2020**, *704*, 135373. [[CrossRef](#)]
15. Mo, K.C.; Lettenmaier, D.P. Heat wave flash droughts in decline. *Geophys. Res. Lett.* **2015**, *42*, 2823–2829. [[CrossRef](#)]
16. Mo, K.C.; Lettenmaier, D.P. Precipitation deficit flash droughts higher risk of flash drought over China. *J. Hydrometeorol.* **2016**, *17*, 1169–1184. [[CrossRef](#)]
17. Ford, T.W.; Labosier, C.F. Meteorological conditions and associated with the onset of flash drought in the Eastern United States. *Agr. Forest Meteorol.* **2017**, *247*, 414–423. [[CrossRef](#)]
18. Anderson, M.; Hain, C.; Otkin, J.; Zhan, X.; Mo, K.; Svoboda, M.; Wardlow, B.D.; Pimstein, A. An Intercomparison of Drought Indicators Based on Thermal Remote Sensing and NLDAS-2 Simulations with U.S. Drought Monitor Classifications. *J. Hydrometeorol.* **2013**, *14*, 1035–1056. [[CrossRef](#)]
19. Noguera, I.; Domínguez-Castro, F.; Vicente-Serrano, S.M. Characteristics and trends of flash droughts in Spain, 1961–2018. *Ann. N. Y. Acad. Sci.* **2019**, *1472*, 155–172. [[CrossRef](#)] [[PubMed](#)]
20. Liu, Y.; Zhu, Y.; Ren, L.L.; Al, E. Two different methods for flash drought identification: Comparison of their strengths and limitations. *J. Hydrometeorol.* **2020**, *21*, 691–704. [[CrossRef](#)]
21. Otkin, J.A.; Anderson, M.C.; Hain, C.; Al, E. Assessing the evolution of soil moisture and vegetation conditions during 2012 United States flash drought. *Agr. Forest Meteorol.* **2016**, *218*, 230–242. [[CrossRef](#)]
22. Zhang, L.; Liu, Y.; Ren, L.; Teuling, A.J.; Zhu, Y.; Wei, L.; Zhang, L.; Jiang, S.; Yang, X.; Fang, X.; et al. Analysis of flash droughts in China using machine learning. *Hydrol. Earth Syst. Sci.* **2022**, *26*, 3241–3261. [[CrossRef](#)]
23. Kam, J.; Sheffield, J.; Yuan, X.; Wood, E.F. Did a skillful prediction of sea surface temperatures help or hinder forecasting of the 2012 Midwestern US drought? *Environ. Res. Lett.* **2014**, *9*, 34005. [[CrossRef](#)]
24. Hao, Z.C.; Singh, V.P.; Xia, Y.L. Seasonal drought prediction: Advances, challenges, and future prospects. *Rev. Geophys.* **2018**, *56*, 108–141. [[CrossRef](#)]
25. Paimazumder, D.; Done, J.M. Potential predictability sources of the 2012 U.S. drought in observations and a regional model ensemble. *J. Geophys. Res. Atmos.* **2016**, *121*, 12581–12592. [[CrossRef](#)]
26. Pendergrass, A.G.; Meehl, G.A.; Pulwarty, R.; Hobbins, M.; Hoell, A.; AghaKouchak, A.; Bonfils, C.; Gallant, A.; Hoerling, M.; Hoffmann, D.; et al. Flash droughts present a new challenge for subseasonal-to-seasonal prediction. *Nat. Clim. Change* **2020**, *10*, 191–199. [[CrossRef](#)]
27. Teuling, A.J. A hot future for European droughts. *Nat. Clim. Change* **2018**, *8*, 360–369. [[CrossRef](#)]

28. Wang, L.; Yuan, X.; Xie, Z.; Wu, P.; Li, Y. Increasing flash droughts over China during the recent global warming hiatus. *Sci. Rep.* **2016**, *6*, 30571. [[CrossRef](#)]
29. Hobbins, M.T.; Andrew, W.; Mcevoy, D.J.; Huntington, J.L.; Charles, M.; Martha, A.; Christopher, H. The Evaporative Demand Drought Index. Part I: Linking Drought Evolution to Variations in Evaporative Demand. *J. Hydrometeorol.* **2016**, *17*, 1745–1761. [[CrossRef](#)]
30. Bauer, P.; Thorpe, A.; Brunet, G. The quiet revolution of numerical weather prediction. *Nature* **2015**, *525*, 47–55. [[CrossRef](#)]
31. Su, X.; Yuan, H.; Zhu, Y.; Luo, Y.; Wang, Y. Evaluation of TIGGE ensemble predictions of Northern Hemisphere summer precipitation during 2008–2012. *J. Geophys. Res. Atmos.* **2014**, *119*, 7292–7310. [[CrossRef](#)]
32. Li, W.; Duan, Q.; Miao, C.; Ye, A.; Gong, W.; Di, Z. A review on statistical postprocessing methods for hydrometeorological ensemble forecasting. *Wiley Interdiscip. Rev. Water* **2017**, *4*, e1246. [[CrossRef](#)]
33. Jha, S.K.; Shrestha, D.L.; Stadnyk, T.A.; Coulibaly, P. Evaluation of ensemble precipitation forecasts generated through post-processing in a Canadian catchment. *Hydrol. Earth Syst. Sci.* **2018**, *22*, 1957–1969. [[CrossRef](#)]
34. Cuo, L.; Pagano, T.C.; Wang, Q.J. A Review of Quantitative Precipitation Forecasts and Their Use in Short- to Medium-Range Streamflow Forecasting. *J. Hydrometeorol.* **2011**, *12*, 713–728. [[CrossRef](#)]
35. Zhang, Y.Q.; You, Q.L.; Chen, C.C.; Li, X. Flash droughts in a typical humid and subtropical basin: A case study in the Gan River Basin, China. *J. Hydrol.* **2017**, *551*, 162–176. [[CrossRef](#)]
36. Osman, M.; Zaitchik, B.F.; Badr, H.S.; Christian, J.I.; Tadesse, T.; Otkin, J.A.; Anderson, M.C. Flash drought onset over the contiguous United States: Sensitivity of inventories and trends to quantitative definitions. *Hydrol. Earth Syst. Sci.* **2021**, *25*, 565–581. [[CrossRef](#)]
37. Wu, L.; Seo, D.; Demargne, J.; Brown, J.D.; Cong, S.; Schaake, J. Generation of ensemble precipitation forecast from single-valued quantitative precipitation forecast for hydrologic ensemble prediction. *J. Hydrol.* **2011**, *399*, 281–298. [[CrossRef](#)]
38. Cai, C.; Wang, J.; Li, Z. Assessment and modelling of uncertainty in precipitation forecasts from TIGGE using fuzzy probability and Bayesian theory. *J. Hydrol.* **2019**, *577*, 123995. [[CrossRef](#)]
39. Ma, F.; Luo, L.; Ye, A.; Duan, Q. Drought characteristics and propagation in the semi-arid Heihe River basin in northwestern China. *J. Hydrometeorol.* **2019**, *20*, 59–77. [[CrossRef](#)]
40. Yuan, X.; Wang, L.; Wu, P.; Ji, P. Anthropogenic shift towards higher risk of flash drought over China. *Nat. Commun.* **2019**, *10*, 4661. [[CrossRef](#)]
41. Arnal, L.; Cloke, H.L.; Stephens, E.; Wetterhall, F.; Prudhomme, C.; Neumann, J.; Krzeminski, B.; Pappenberger, F. Skilful seasonal forecasts of streamflow over Europe? *Hydrol. Earth Syst. Sci.* **2018**, *22*, 2057–2072. [[CrossRef](#)]
42. Yun, W.T. *WWRP WWRP/WCRP Sub-Seasonal to Seasonal Prediction Project (S2S) Phase II Proposal*; S2S News Letter; World Meteorological Organization: Geneva, Switzerland, 30 March 2018.
43. Bougeault, P.; Toth, Z.; Bishop, C.; Brown, B.; Burridge, D.; Chen, D.H.; Ebert, B.; Fuentes, M.; Hamill, T.M.; Mylne, K.; et al. The THORPEX Interactive Grand Global Ensemble. *Bull. Am. Meteorol. Soc.* **2010**, *91*, 1059–1072. [[CrossRef](#)]
44. Yuan, X.; Wood, E.F. Multimodel seasonal forecasting of global drought onset. *Geophys. Res. Lett.* **2013**, *40*, 4900–4905. [[CrossRef](#)]
45. Seager, R.; Hoerling, M. Atmosphere and ocean origins of North American droughts. *J. Climate* **2014**, *27*, 4581–4606. [[CrossRef](#)]
46. Schubert, S.D.; Stewart, R.E.; Wang, H.; Berbery, E.H.; Cai, W.; Hoerling, M.P.; Kanikicharla, K.K.; Koster, R.D.; Lyon, B.; Mariotti, A.; et al. Global Meteorological Drought: A Synthesis of Current Understanding with a Focus on SST Drivers of Precipitation Deficits. *J. Climate* **2016**, *29*, 3989–4019. [[CrossRef](#)]
47. Cai, C.; Wang, J.; Li, Z. Improving TIGGE Precipitation Forecasts Using an SVR Ensemble Approach in the Huaihe River Basin. *Adv. Meteorol.* **2018**, *2018*, 1–15. [[CrossRef](#)]
48. Cai, C.; Wang, J.; Li, Z.; Shen, X.; Wen, J.; Wang, H.; Wu, C. A New Hybrid Framework for Error Correction and Uncertainty Analysis of Precipitation Forecasts with Combined Postprocessors. *Water* **2022**, *14*, 3072. [[CrossRef](#)]

Disclaimer/Publisher’s Note: The statements, opinions and data contained in all publications are solely those of the individual author(s) and contributor(s) and not of MDPI and/or the editor(s). MDPI and/or the editor(s) disclaim responsibility for any injury to people or property resulting from any ideas, methods, instructions or products referred to in the content.